# ANTICRACK NUCLEATION IN SNOWPACKS WITHOUT ASSUMING INITIAL DEFECTS: MODELING DRY SNOW SLAB AVALANCHES

Philipp L. Rosendahl[1,2,*], Vera Lübke[2], Philipp Weißgraeber[1,3,*]

[1] 2$\varphi$, www.2phi.de, Darmstadt, Germany
[2] Technische Universtität Darmstadt, Fachgebiet Strukturmechanik, Darmstadt, Germany
[3] Robert Bosch GmbH, Corporate Research and Advance Engineering, Renningen, Germany

ABSTRACT: To improve modeling of slab avalanche release we propose a new mechanical snowpack model and a novel criterion for anticrack nucleation. The model allows to analyze skier-loaded slopes as well as PST experiments. We obtain closed-form analytical expressions for shear and normal stresses in the weak layer as well as for the energy release rate of cracks, which are in very good agreement with finite element analyses.

In this work, a new conceptual understanding of the fracture initiation process of dry snow slab avalanches is developed. It makes use of the coupled stress and energy criterion in the framework of finite fracture mechanics. No assumption of initial flaw size is required. The initiation of defects and subsequent crack propagation is covered by a single criterion containing both a strength of materials and a fracture mechanics condition.

*Keywords:* slab avalanche release, fracture mechanics, predictive modeling, snowpack model

## 1. INTRODUCTION

The release of snow slab avalanches is preceded by fracture processes within the snowpack (Schweizer et al., 2016). A crack nucleates within a porous and compressible persistent weak layer of faceted crystals or hoar under the snow slab. It propagates across the slope and creates a surface for the slab to slide on. Based on stress and strength considerations a stability index was proposed by Föhn (1987) and improved by Jamieson and Johnston (1998). McClung (1979) used a fracture mechanics model for propagation of defects initiated by ductile shear failure. Chiaia et al. (2008) added the consideration of energy balance to the modeling of shear failure.

A new understanding of weak layer collapse as the snowpack failure mechanism was given by Heierli et al. (2008). They introduced the anticrack model, which additionally considers slope normal deformations. It provides physical explanation for "whumpf" sounds often encountered in avalanche terrain. Capturing crack propagation within the weak layer is understood as a key element of failure modeling (van Herwijnen and Jamieson (2007); Gaume et al. (2015, 2017)). Mixed-mode interaction of shear and normal stresses was studied by Reiweger et al. (2015). Inspired by this criterion Gaume et al. (2017, 2018) use numerical simulations to compute critical crack lengths and dynamic anticrack propagation. The effect of snowpack layering on the fracture process was considered by Reuter et al. (2015), Monti et al. (2015) as well as Gaume and Reuter (2017).

A new in-situ experiment allowing for quantitative analyses of the fracture properties of the snow slab was developed with the propagation saw test (PST) (Gauthier and Jamieson, 2006; Sigrist and Schweizer, 2007). The test provides insight into the fracture processes in snowpacks. Benedetti et al. (2018) proposed a beam model for stress-based analyses of critical cut lengths. The results of PST experiments were used to discuss shear fracture zones (McClung, 2009) and to propose new methods for estimating snowpack instability (Reuter et al., 2015).

Many of the above models use overly simplified assumptions leading to incomplete representations of deformation and stress fields. Important effects such as the deformation of the weak layer are not accounted for, although they were shown to be of major importance (Reiweger and Schweizer, 2010). None of the given models provides a comprehensive picture of avalanche release as a unified failure process which is controlled by overloading (strength) and energy requirements of the crack (toughness).

In this work, we propose a novel model for the nucleation of anticracks by means of a coupled stress and energy criterion. To employ this criterion a new comprehensive snowpack model is proposed which allows for closed-form computation of the normal and shear stress in the weak layer as well as the energy release rate of cracked weak layers. The model is then used to evaluate the new coupled stress and energy failure criterion for anticrack nucleation in snow packs without assuming initial defects.

## 2. MECHANICAL SNOWPACK MODEL

Consider the snowpack depicted in Fig. 1a. Following the idea of Heierli et al. (2008) the snow slab is modeled as a plane strain Timoshenko beam with out-of

*Corresponding authors' address: mail@2phi.de

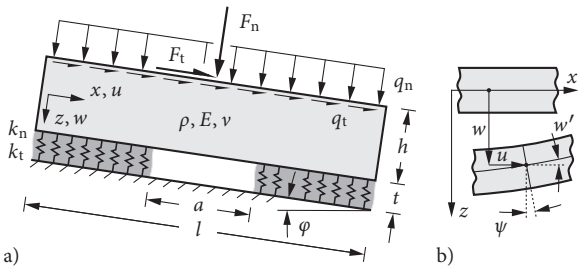


Figure 1: Snowpack modeled a) as a beam on an elastic foundation of an infinite set of shear and compressive springs b) using Timoshenko beam kinematics.

plane thickness $b$. In the present model an elastic foundation of an infinite set of smeared springs is added representing the weak layer. The springs possess compressive $k_n$ and shear stiffness $k_t$.

Displacements of the snow slab are described by a set of linear differential equations with constant coefficients. The horizontal displacement $u$ is obtained from

$$EAu''(x) - k_t u(x) + q_t = 0, \tag{1}$$

where the extension stiffness $EA$ is composed of the Young's modulus $E$ and the snow slab cross section $A = hb$. $k_t = G_{wl} b/t$ is the weak layer shear stiffness with the shear modulus $G_{wl} = E_{wl}/(2(1+\nu))$ and $q_t = \rho g h b \sin(\varphi)$ is a constant distributed horizontal load in $x$-direction.

The vertical beam deflection $w$ and the rotation of the beam cross section $\psi$ are coupled through (e.g. Hetenyi, 1946; Timoshenko and Goodier, 1951)

$$EIw''''(x) - \frac{k_n}{\kappa GA} w''(x) + \frac{k_n}{EI} w(x) = \frac{q_n}{EI}, \tag{2}$$

$$\psi(x) = -\frac{EI}{\kappa GA} w'''(x) + \left( \frac{EI\, k_n}{(\kappa GA)^2} - 1 \right) w'(x), \tag{3}$$

where $\kappa = 5/6$ is the shear correction factor for rectangular cross sections, $I = bh^3/12$ the moment of inertia, $k_n = E_{wl} b/t$ the weak layer compressive stiffnesses and $q_n = \rho g h b \cos(\varphi)$ a constant distributed vertical load in $z$-direction.

The general solution of the ODE (1) for the horizontal displacement is

$$u(x) = c_1 \cosh(\mu x) + c_2 \sinh(\mu x) + \frac{q_t}{k_t}, \tag{4}$$

where $\mu = \sqrt{k_t/(EA)}$ is the corresponding eigenvalue and $c_1$ and $c_2$ are constants which must be determined from boundary conditions. The solution of the coupled ODEs (2) and (3) is of exponential type as well. Depending on the material parameters, the eigenvalues of this solution may become real or complex. The respective solutions with eigenvalues $\lambda_{1,2}$ and $\lambda^*_{1,2}$ are

$$\begin{aligned} w(x) = {} & c_1 \cosh(\lambda_1 x) + c_2 \sinh(\lambda_1 x) \\ & + c_3 \cosh(\lambda_2 x) + c_4 \sinh(\lambda_2 x) + \frac{q_n}{k_n}, \end{aligned} \tag{5}$$

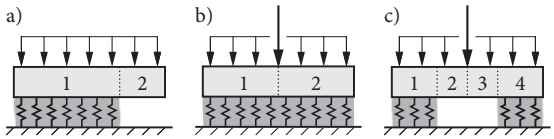


Figure 2: Snowpack configurations assembled from beam segments with boundary and transmission conditions: a) PST b) skier load on intact weak layer c) skier load on weak layer with crack. Weak layer cracks are modeled by removing support of the beam. For the sake of clarity only vertical loads are shown.

for real eigenvalues, when $k_n EI \geq 4(\kappa GA)^2$, and

$$\begin{aligned} w(x) = {} & e^{\lambda_1^* x} \left( c_1 \cos(\lambda_2^* x) + c_2 \sin(\lambda_2^* x) \right) \\ & + e^{-\lambda_1^* x} \left( c_3 \cos(\lambda_2^* x) + c_4 \sin(\lambda_2^* x) \right) + \frac{q_n}{k_n}, \end{aligned} \tag{6}$$

for complex eigenvalues, when $k_n EI < 4(\kappa GA)^2$. Again, the constants $c_1$ to $c_4$ must be determined from boundary conditions.

Snowpack configurations can be assembled from beam segments with elastic foundation or without ($k_t = k_n = 0$, Heierli's solution). Modeling a propagation saw test requires two beam segments as shown in Fig. 2a. The left part of the snow slab rests on an elastic foundation representing the intact weak layer. The right part is a cantilever beam where cutting has removed the weak layer support. The slab is loaded by its own weight $q_n$ and $q_t$. Free left and right ends require vanishing section forces and moments. At the transition between the unsupported and supported segments $C^0$-continuity of displacements, cross section rotation and section forces and moments is enforced. When concentrated forces (skier load) are to be considered (Figs. 2b and 2b), the discontinuity of normal and transverse shear forces must be accounted for.

The boundary and transmission conditions for the respective load case provide a linear system of equations with up to 18 unknown constants. The system can be solved easily (<1 ms on a standard desktop PC) using common mathematical toolboxes. Closed-form solutions for $u$, $w$ and $\psi$ can be given.

Because of the simple weak layer kinematics, known slab displacements automatically yield weak layer compressive and shear stresses according to

$$\sigma(x) = -\frac{k_n}{b} w(x), \qquad \tau(x) = \frac{k_t}{b} u(x). \tag{7}$$

Further, denoting the total potential energy as $\Pi$ the energy release rate

$$\mathcal{G} = -\frac{d\Pi}{b\,da} = \mathcal{G}_I + \mathcal{G}_{II}, \tag{8}$$

for a weak layer crack of length $a$ is given by

$$\mathcal{G}_I = \frac{k_n}{2b} w(a)^2, \qquad \mathcal{G}_{II} = \frac{k_t}{2b} u(a)^2, \tag{9}$$

where $w(a)$ and $u(a)$ correspond to displacements at the crack tip (Krenk, 1992). That is, the energy

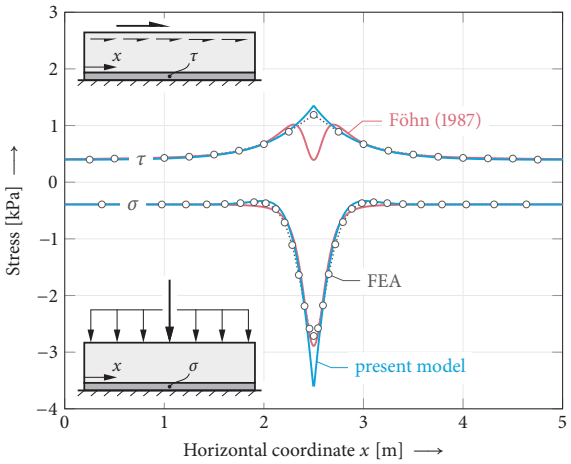


Figure 3: Normal and shear stresses from combined skier and slab weight loading. Comparison of present model (blue) and Föhn (1987) model (red) to FEA results (circles). The following material and geometry parameters are used: $l = 5\,\mathrm{m}$, $b = 1\,\mathrm{mm}$, $h = 200\,\mathrm{mm}$, $t = 10\,\mathrm{mm}$, $\rho = 200\,\mathrm{kg/m^3}$, $E_{\mathrm{slab}} = 5\,\mathrm{MPa}$, $E_{\mathrm{wl}} = 0.15\,\mathrm{MPa}$, $\nu = 0.25$, $q_{\mathrm{n}} = q_{\mathrm{t}} = 0.39$ kPa, $F_{\mathrm{n}} = F_{\mathrm{t}} = 0.78\,\mathrm{N}$.

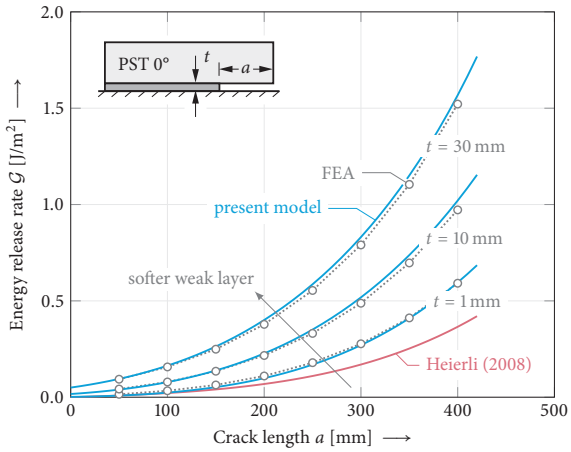


Figure 4: PST energy release rate $\mathcal{G}$ in flat terrain. Comparison of present model (blue lines), Heierli (2008) model (red line) and FEA results (gray circles). Both models agree well with FEA data for short crack lengths and stiff (i.e. thin) weak layers. While (Heierli, 2008) cannot reproduce varying weak layer properties, the present model exhibits excellent agreement with FEA results. The following material and geometry parameters are used: $l = 1200\,\mathrm{mm}$, $h = b = 300\,\mathrm{mm}$, $E_{\mathrm{wl}} = 0.15\,\mathrm{MPa}$, $\nu = 0.17$, $\rho = 240\,\mathrm{kg/m^3}$ and $E_{\mathrm{slab}}$ calculated according to Scapozza (2004).

release rate can be interpreted as the energy stored in the (shear and normal) springs at the crack tip.

## 3. VALIDATION OF THE MECHANICAL SNOWPACK MODEL

The present model provides slab displacements, weak layer stresses and energy release rates for cracks within the weak layer as closed-form analytical expressions. In order to validate the model, stresses and energy release rates are compared against detailed plane strain finite element analyses (FEA) and existing models. To investigate the capabilities of the present model we compute the fracture toughness at the measured crack onset in propagation saw tests (PST) for a comprehensive set of 93 field experiments provided by Gaume et al. (2017). For the following considerations, the Young's modulus is calculated from density $\rho$ using the empirical relation of Scapozza (2004) in plane strain conditions.

Fig. 3 shows weak layer compressive and shear stresses for combined skier and gravity loading calculated using FEA, equations given by Föhn (1987) and the present model. Föhn's solution for a force acting on an elastic halfplane and the present model both show a good agreement with the FEA results.

Fig. 4 shows energy release rates for PSTs in flat terrain. The anticrack model by Heierli (2008) and the present model are compared against FEA results for different weak layer thicknesses. FEA energy release rates are approximated using the central difference quotient

$$\mathcal{G}(a) = -\frac{\mathrm{d}\Pi}{b\mathrm{d}a} \approx -\frac{\Delta\Pi(a+\delta) - \Delta\Pi(a-\delta)}{b\,2\delta}, \qquad (10)$$

where $\delta$ is a small crack increment and $\Delta\Pi$ is the difference in total potential energy between cracked and uncracked configuration. A crack is introduced removing all weak layer elements on the length $a$.

Heierli's model assumes a rigid weak layer which corresponds to a beam resting on an indefinitely thin weak layer yet permitting beam deflections. With thicker weak layers, the weak layer compliance increases and Heierli's assumption of rigidity leads to increasing discrepancies. This is reflected in Fig. 4. For short cracks and thin weak layers Heierli's model agrees well with FEA results. However, the energy release rate of soft weak layers and long cracks is only predicted correctly by the present model which accounts for weak layer deformation.

Fig. 5 correlates model predictions for the weak layer fracture toughness to data obtained using detailed FEAs and Eq. (10). Fracture toughnesses $\mathcal{G}_{\mathrm{c}}$ are determined from critical cut lengths $a_{\mathrm{c}}$ measured in 93 PST field experiments. Because Heierli's model neglects weak layer deformations, it underestimates the fracture toughness significantly (see Fig. 4). It neither shows a satisfactory slope of the linear regression nor a reasonable coefficient of determination $R^2$. Predictions of the present model are found within a narrow range around the one-to-one line.

## 4. FINITE FRACTURE MECHANICS CRITERION FOR SKIER-TRIGGERED ANTICRACKS

Typically it is assumed that the formation of defects occurs because of other mechanisms (stress and strength) or even on different time scales (McClung, 1979) than propagation of cracks in the slope (frac-

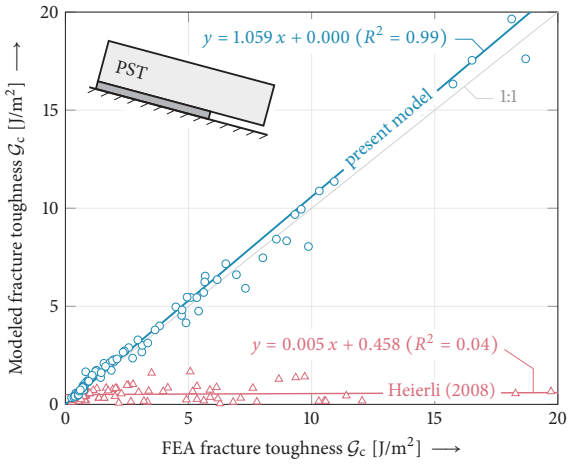


Figure 5: Modeled fracture toughness $\mathcal{G}_c$ versus fracture toughness obtained using FEAs for material properties determined in 93 field PSTs. Comparison of data points, linear regression and coefficient of determination $R^2$ of present model (blue) and Heierli (2008) model (red). No data set showed the slab touching the substratum.

ture mechanics). Fracture mechanics approaches are restricted to pre-existing cracks and hence cannot be used to model crack initiation. The question of critical crack sizes required for instable crack propagation arises and if load-induced defects which are too small to propagate persist in the snowpack.

This can be resolved by simultaneously requiring both the weak layer to be overloaded in terms of stress and to have sufficient energy available for the formation of new crack surfaces. In general form this criterion can be given as:

$$\begin{cases} f(\sigma,\tau) & \geq & 1 & \text{on } \Delta a \text{ prior to fracture,} \\ \overline{\mathcal{G}}(\Delta a) & \geq & \mathcal{G}_c & \text{at fracture.} \end{cases} \tag{11}$$

This so called coupled stress and energy criterion is known in the framework of finite fracture mechanics and has proven useful for studying crack initiation in many engineering structural situations with brittle materials (Weißgraeber et al., 2016). It provides critical loads as well as the size of initiating cracks and thus does not require the assumption of initial defects. The concept requires only the two fundamental material properties strength and fracture toughness as input. Similar thoughts were presented by Chiaia et al. (2008) for snowpack shear failure. The principles of the coupled criterion are shown in Fig. 6. Here, both conditions which must be fulfilled simultaneously are shown schematically for the case of a skier loaded snowpack.

Using the coupled criterion Eq. (11) requires a strength hypothesis. To account for mixed-mode interaction of shear and normal stress a quadratic stress interaction is considered:

$$f(\sigma,\tau) = \sqrt{\left(\frac{\sigma}{\sigma_c}\right)^2 + \left(\frac{\tau}{\tau_c}\right)^2} \geq 1, \tag{12}$$

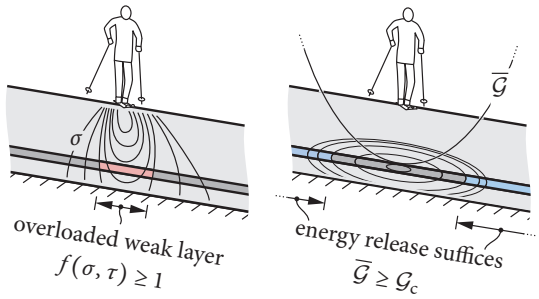


Figure 6: Evaluation of the coupled stress and energy criterion for the case of skier loaded snowpack. On the left the condition of a locally overloaded weak layer and on the right the second condition of sufficient energy release rate are shown. The stress condition has the effect of an upper bound on possible nucleated cracks. Whereas the energy condition provides a lower bound on the crack lengths as short cracks do not release sufficient energy.

where $\tau_c$ is the effective shear strength according to Reiweger et al. (2015) which depends on the compressive stress $\sigma$.

The second condition considers the energy release rate of finite cracks $\overline{\mathcal{G}}$. It can be obtained by integrating the differential energy release rate $\mathcal{G}$ over the finite crack length $\Delta a$ or by evaluating the corresponding change of the total potential $\Delta\Pi$:

$$\overline{\mathcal{G}} = \frac{1}{\Delta a}\int_{\Delta a} \mathcal{G}\,\mathrm{d}a = -\frac{\Delta\Pi}{b\Delta a} = \overline{\mathcal{G}}_{\mathrm{I}} + \overline{\mathcal{G}}_{\mathrm{II}}. \tag{13}$$

In this work, the change of the total potential is evaluated by means of the crack opening integral. The change of total potential equals the work done by stresses on crack flanks when reduced quasi-statically to zero (which corresponds to crack opening). This can be done for both mode I and mode II contributions and the following relations of the incremental energy release rates are obtained:

$$\begin{aligned} \overline{\mathcal{G}}_{\mathrm{I}} &= \frac{1}{2b\Delta a}\int_{\frac{l-\Delta a}{2}}^{\frac{l+\Delta a}{2}} k_{\mathrm{n}} w_1(x)\, w_0(x)\,\mathrm{d}x, \\ \overline{\mathcal{G}}_{\mathrm{II}} &= \frac{1}{2b\Delta a}\int_{\frac{l-\Delta a}{2}}^{\frac{l+\Delta a}{2}} k_{\mathrm{t}} u_1(x)\, u_0(x)\,\mathrm{d}x, \end{aligned} \tag{14}$$

where indices 0 and 1 refer to uncracked and cracked configurations, respectively.

By using Eqs. (12) and (13) in the coupled stress and energy criterion Eq. (11) one obtains a set of two implicit equations with two unknowns: the critical load and the finite size of the initiated defect. This set of equations can be readily solved with standard numerical toolboxes (with computation times <5 ms).

Results of a parametric study of this coupled stress and energy criterion are shown in Fig. 7. A snowpack loaded by its weight and an additional line load (representing e.g. a skier) is considered and the critical additional load which causes anticrack nucleation is calculated. The dependence of this load on the height of the superstratum is shown. With increasing

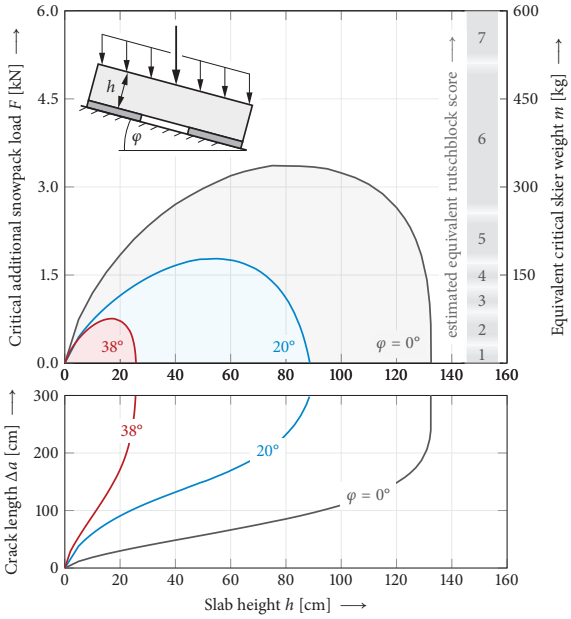


Figure 7: Critical snowpack loading and size of initiated anticracks as a function of slab height. Thicker slabs transfer concentrated loads more uniformly allowing for larger point loads. Above a certain thickness, failure is dominated by the slab's own weight reducing admissible additional loads until self release occurs. The following material and geometry parameters are used: $t = 5$ mm, $E_{\mathrm{slab}} = 5$ MPa, $E_{\mathrm{wl}} = 0.15$ MPa, $\nu = 0.25$, $\rho = 200$ kg/m$^3$, $l = 25h$, $\mathcal{G}_{\mathrm{c}} = 3.0$ J/m$^2$ (median of PST field data used in present work).

slab thickness the load bearing capacity increases as the increasing stiffness of the slab leads to a more uniform load distribution. However, at a certain slab thickness the effect of the increasing slab weight outweighs the former effect and the capacity to bear additional load reduces. At a threshold thickness self release without additional load occurs. The results are given for three different slope angles yielding decreasing critical loads on steeper slopes. In the subplot below sizes of nucleated anticracks are shown agreeing well the estimates given by Schweizer (1999) or Gaume et al. (2017). For the case of self-release the length of the nucleated cracks tends to infinity as no zone of local overloading exists. Critical load predictions of the present model could be validated using rutschblock test data. To this end, we provide estimates for load-equivalent rutschblock scores assuming a skier weight of 85 kg.

## 5. CONCLUSION

The present analysis shows that the consideration of weak layer deformations is crucial in the mechanical modeling of snowpacks. Our model provides closed-form solutions for weak layer stresses and energy release rates which are in very good agreement with finite element results. In combination with PST field tests it allows for reliably determining the weak layer fracture toughness. Within the present framework layered snow slabs can be considered using laminated beam theory in future works.

The presented coupled stress and energy failure criterion demonstrates that both stress and energy are necessary conditions for the initiation of cracks. It provides a physically sound explanation for anticrack nucleation without requiring assumptions on initial defects and predicts admissible skier loads.

## ACKNOWLEDGEMENTS

We thank Johan Gaume and Alec van Herwijnen for helpful discussions and providing PST field data.

## REFERENCES

Benedetti, L., Gaume, J., and Fischer, J.-T. (2018). *International Journal of Solids and Structures. Article in press.*

Chiaia, B. M., Cornetti, P., and Frigo, B. (2008). *Cold Regions Science and Technology*, 53(2):170–178.

Föhn, P. M. B. (1987). *Avalanche Formation, Movement and Effects*, 162:195–214.

Gaume, J., Gast, T., Teran, J., van Herwijnen, A., and Jiang, C. (2018). *Nature Communications*, 9(1):3047.

Gaume, J. and Reuter, B. (2017). *Cold Regions Science and Technology*, 144(May):6–15.

Gaume, J., van Herwijnen, A., Chambon, G., Birkeland, K. W., and Schweizer, J. (2015). *The Cryosphere*, 9(5):1915–1932.

Gaume, J., van Herwijnen, A., Chambon, G., Wever, N., and Schweizer, J. (2017). *The Cryosphere*, 11(1):217–228.

Gauthier, D. and Jamieson, B. (2006). *Journal of Glaciology*, 52(176):164–168.

Heierli, J. (2008). *Anticrack model for slab avalanche release*. PhD thesis, Universität Karlsruhe.

Heierli, J., Gumbsch, P., and Zaiser, M. (2008). *Science*, 321(5886):240–243.

Hetenyi, M. (1946). *Beams on elastic foundations*. The University of Michigan Press, Ann Arbor, Michigan.

Jamieson, J. B. and Johnston, C. D. (1998). *Annals of Glaciology*, 26:296–302.

Krenk, S. (1992). *Eng. Fracture Mechanics*, 43(4):549–559.

McClung, D. M. (1979). *Journal of Geophysical Research*, 84(B7):3519–3526.

McClung, D. M. (2009). *Journal of Geophysical Research*, 114(F1):F01022.

Monti, F., Gaume, J., van Herwijnen, A., and Schweizer, J. (2015). *Natural Hazards and Earth System Sciences Discussions*, 3(8):4833–4869.

Reiweger, I., Gaume, J., and Schweizer, J. (2015). *Geophysical Research Letters*, 42(5):1427–1432.

Reiweger, I. and Schweizer, J. (2010). *Geophysical Research Letters*, 37(24):L24501.

Reuter, B., Schweizer, J., and Van Herwijnen, A. (2015). *Cryosphere*, 9(3):837–847.

Scapozza, C. (2004). *Entwicklung eines dichte- und temperaturabhängigen Stoffgesetzes zur Beschreibung des viskoelastischen Verhaltens von Schnee*. PhD thesis, ETH Zürich.

Schweizer, J. (1999). *Cold Regions Science and Technology*, 30(1-3):43–57.

Schweizer, J., Reuter, B., van Herwijnen, A., and Gaume, J. (2016). In *Proceedings ISSW, Breckenridge, Colorado*, pages 1–11.

Sigrist, C. and Schweizer, J. (2007). *Geophysical Research Letters*, 34(3).

Timoshenko, S. and Goodier, J. N. (1951). *Theory of Elasticity*. McGraw-Hill, 2 edition.

van Herwijnen, A. and Jamieson, B. (2007). *Cold Regions Science and Technology*, 50(1-3):13–22.

Weißgraeber, P., Leguillon, D., and Becker, W. (2016). *Archive of Applied Mechanics*, 86(1-2):375–401.